The O-glycan pathway is associated with *in vitro* sensitivity to gemcitabine and overall survival from ovarian cancer

NADIM BOU ZGHEIB[1], YIN XIONG[1,2], DOUGLAS C. MARCHION[1,2], ELONA BICAKU[1,2], HYE SOOK CHON[1], XIAOMANG BA STICKLES[1], ENTIDHAR AL SAWAH[1], PATRICIA L. JUDSON[1,4], ARDESHIR HAKAM[3,4], JESUS GONZALEZ-BOSQUET[1,4], ROBERT M. WENHAM[1,2,4], SACHIN M. APTE[1,4], CHRISTOPHER L. CUBITT[5], DUNG TSA CHEN[6] and JOHNATHAN M. LANCASTER[1,2,4]

[1]Department of Women's Oncology, [2]Experimental Therapeutics Program, [3]Department of Anatomic Pathology, [4]Department of Oncologic Sciences at the University of South Florida, [5]Translational Research and [6]Biostatistics Core, H. Lee Moffitt Cancer Center and Research Institute, Tampa, FL 33612, USA

Received January 9, 2012; Accepted March 16, 2012

DOI: 10.3892/ijo.2012.1451

Abstract. Ovarian cancer (OVCA) is the most lethal gynecological malignancy. The high mortality rate associated with this disease is due in large part to the development of resistance to chemotherapy; however, the biological basis of this remains unclear. Gemcitabine is frequently used for the treatment of patients with platinum-resistant OVCA. We report molecular signaling pathways associated with OVCA response to gemcitabine. Forty-one OVCA cell lines were subjected to gene expression analysis; in parallel, IC_{50} values for gemcitabine were quantified using CellTiter-Blue viability assays. Pearson's correlation coefficients were calculated for gene expression and gemcitabine IC_{50} values. The genes associated with gemcitabine sensitivity were subjected to pathway analysis. For the identified pathways, principal component analysis was used to derive pathway signatures and corresponding scores, which represent overall measures of pathway expression. Expression levels of the identified pathways were then evaluated in a series of clinico-genomic datasets from 142 patients with stage III/IV serous OVCA. We found that *in vitro* gemcitabine sensitivity was associated with expression of 131 genes ($p<0.001$). These genes include significant representation of three molecular signaling pathways ($p<0.02$): O-glycan biosynthesis, Role of Nek in cell cycle regulation and Antiviral actions of Interferons. In an external clinico-genomic OVCA dataset (n=142), expression of the O-glycan pathway was associated with overall survival, independent of surgical cytoreductive status, grade and age ($p<0.001$). Expression levels of Role of Nek in cell cycle regulation and Antiviral actions of Interferons were not associated with survival ($p=0.31$ and $p=0.54$, respectively). Collectively, expression of the O-glycan biosynthesis pathway, which modifies protein function via post-translational carbohydrate binding, is independently associated with overall survival from OVCA. Our findings shed light on the molecular basis of OVCA responsiveness to gemcitabine and also identify a signaling pathway that may influence patient survival.

Correspondence to: Dr Johnathan M. Lancaster, Center for Women's Oncology, Department of Women's Oncology, Moffitt Cancer Center, 12902 Magnolia Drive, Tampa, FL 33612, USA
E-mail: johnathan.lancaster@moffitt.org

Key words: gemcitabine chemosensitivity, genomic study, O-glycan pathway, principal component analysis, ovarian cancer survival

Introduction

Ovarian cancer (OVCA) is the leading cause of gynecologic cancer mortality and the sixth most common cancer diagnosed in women in the United States. Advanced-stage epithelial OVCA is highly heterogeneous at a clinical, biologic, and genetic level, but patients are currently treated in a uniform fashion with cytoreductive surgery and platinum/taxane-based combination chemotherapy. Unfortunately, most patients ultimately succumb to persistent or recurrent platinum-resistant disease (1,2). Currently, efforts to develop therapeutic agents with greater efficacy against platinum-resistant disease are limited because of an incomplete understanding of the molecular determinants of OVCA drug response.

Gemcitabine (2',2'-difluorodeoxycytidine), a synthetic nucleoside analog of cytidine, is frequently used as a second-line therapy for patients with relapsed OVCA (3). As a pyrimidine analogue, gemcitabine replaces the nucleic acid cytidine during DNA replication, blocking processing and chain elongation by the DNA polymerase complex, resulting in G1 arrest and a subsequent cytostatic effect. Additionally, the gemcitabine triphosphate metabolite is incorporated into RNA, thus inhibiting RNA synthesis (4). Gemcitabine efficacy has been evaluated extensively both *in vitro* and *in vivo* against OVCA (5-8). Gemcitabine has demonstrated single-agent activity against OVCA cell lines (9) and synergistic activity with several other antineoplastic agents, including platinum compounds, topotecan, and etoposide (10). In animal tumor models, the gemcitabine effect has been shown to be schedule dependent, and continuous infusions over 24 h

appear to enhance gemcitabine cytotoxicity (11). Phase II and III studies of gemcitabine (800-1250 mg/m^2/week) in patients with recurrent OVCA have demonstrated response rates up to 19% (12-14). Despite such data, the molecular determinants of gemcitabine activity remain to be fully elucidated. In this study, we sought to determine the molecular underpinnings of OVCA response to gemcitabine at a genome-wide level. We investigated the genes and molecular signaling pathways associated with the response of OVCA cells *in vitro* to gemcitabine and explored how these pathways influence *in vivo* clinical outcomes for patients with this disease.

Materials and methods

Overview. We subjected 41 OVCA cell lines to gene expression analysis and, in parallel, measured gemcitabine sensitivity (IC_{50}). Genes associated with baseline gemcitabine sensitivity, identified by Pearson's correlation analysis, were subjected to molecular pathway analysis. We evaluated expression of identified pathways using a series of clinico-genomic datasets from 142 patients with stage III/IV serous OVCA. All 142 patients had signed IRB-approved, written informed consent forms.

Cell culture. OVCA cell lines were obtained from the American Type Culture Collection (Manassas, VA; CAOV3, OV90, OVCAR3, SKOV3), from the European Collection of Cell Cultures (Salisbury, UK; A2780CP, A2780S), from Kyoto University (Kyoto, Japan; CHI, CHIcisR, M41, M41CSR, Tyknu, and TyknuCisR), or as kind gifts from Dr Patricia Kruk, Department of Pathology, College of Medicine, University of South Florida, Tampa, FL, and Susan Murphy, PhD, Department of OBGYN/Division of GYN Oncology, Duke University, Durham, NC (A2008, C13, CAOV2, HeyA8, IGR-OV1, IMCC3, IMCC5, MCAS, OV2008, OVCA420, OVCA429, OVCA432, OVCA433, FUOV1, PEO1, PEO4, SK-OV-6, T8, TOV-112D, TOV-21-G, Dov13, BG1, Ovary1847, OVCAR10, OVCAR8, OVCAR5, OVCAR4, OVCAR2, SK-OV-4). Cell lines were maintained in RPMI-1640 medium (Invitrogen, Carlsbad, CA) supplemented with 10% fetal bovine serum (Fisher Scientific, Pittsburgh, PA), 1% sodium pyruvate, 1% penicillin/streptomycin (Cellgro, Manassas, VA), and 1% non-essential amino acids (HyClone, Hudson, NH). Mycoplasma testing was performed every 6 months, in accordance with the manufacturer's protocol (Lonza, Rockland, ME).

RNA extraction and microarray expression analysis. RNA from 41 OVCA cell lines was extracted using the RNeasy kit following manufacturer's recommendations (Qiagen, Valencia, CA). Quality of the RNA was measured using an Agilent 2100 Bioanalyzer. The targets for Affymetrix DNA microarray analysis were prepared according to the manufacturer's instructions, and targets were hybridized to customized Human Affymetrix HuRSTA gene chips (HuRSTA-2a520709), which include 60,607 probe sets and representation of 19,308 genes (Gene Expression Omnibus accession number GSE34615).

CellTiter-Blue cell viability assays. Drug activity was evaluated using a high-throughput CellTiter-Blue cell viability assay. Cells ($2.5x10^3$ per well) were plated in 384-well plates using complete media with 10% fetal bovine serum and allowed to adhere overnight. After cell adherence, increasing concentrations of gemcitabine were added to appropriate wells using an automated pipetting station. Four replicate wells were used for each drug concentration and for vehicle controls. Drug dilutions initially consisted of 1.5-fold serial dilutions from a maximum concentration of 100 μM. The cells were incubated with the drug for 72 h, and 5 μl of CellTiter-Blue reagent (Promega Corp.) were added to each well. Fluorescence was read at 579-nm excitation/584-nm emission using a Synergy 4 microplate reader (Bio-Tek Instruments, Inc., Winooski, VT). IC_{50} values were determined using a sigmoidal equilibrium model fit (XLfit 5.2, ID Business Solutions Ltd.). The IC_{50} was defined as the concentration of drug required for a 50% reduction in growth/viability.

Statistical analysis. Expression data from 41 OVCA cell lines were subjected to background correction and normalization using the 'Robust Multichip Average' algorithm in the Affymetrix Expression Console (http://www.affymetrix.com/estore/index.jsp). Pearson's correlation test was performed on individual gene expression and IC_{50} values. Probe sets with $p<0.001$ were considered to have significant correlations with IC_{50} values and were uploaded to MetaCore GeneGo for pathway analysis (http://www.genego.com/metacore.php). Pathways with $p<0.05$ were considered significant, based upon the GeneGo/MetaCore™ statistical test for significance.

Building signatures of pathway activity. The principal component analysis (PCA) methodology was used to derive a gene expression signature for each pathway. A corresponding 'pathway score' was thus generated that quantifies the overall level of pathway gene expression in a summary value. That is, the PCA score is a numeric value that summarizes the level of expression of the entire pathway. First, data were reduced into a small set of uncorrelated principal components. This set of principal components was generated based on its ability to account for variation. The first PCA was used to represent the overall expression level for the pathway as it accounts for the largest variability in the data. That is, the pathway score is equal to $\sum w_i x_i$, a weighted average expression among the pathway genes, where x_i represents gene i expression level, w_i is the corresponding weight (loading coefficient) with $\sum w^2_i=1$, and the w_i values maximize the variance of $\sum w_i x_i$. Details of this methodology have been previously reported by our group (15,16).

Validation of signatures in primary OVCA datasets. The pathway gene expression signature scores were evaluated in an independent publicly available clinico-genomic dataset from 142 OVCA samples (16). In brief, all 142 samples were known to have been resected from patients with advanced-stage (III/IV), serous epithelial OVCA, who underwent primary cytoreductive surgery followed by primary therapy with a platinum-based regimen (+/- taxane or cyclophosphamide). Response to this primary therapy [complete response (CR) versus incomplete response (IR)] has previously been described for these patients (16). In brief, patients who demonstrated a CR had no evidence of disease on physical examination, serum tumor marker monitoring, or radiographic imaging. The IR category included all other patients. Log-rank tests with Kaplan-Meier survival

Table I. Gemcitabine IC_{50}.

Cell line	IC_{50} (mean)	IC_{50} (SD)	No. of cells
A2008	163.9E-9	309.0E-9	12
A2780CP	366.4E-9	696.6E-9	9
A2780S	51.8E-9	46.5E-9	4
BG1	30.4E-6	27.6E-6	8
C13	418.1E-9	804.0E-9	9
CAOV2	3.9E-6	8.5E-6	12
CAOV3	2.2E-9	1.2E-9	5
CHI	268.6E-9	522.6E-9	26
CHIcisR	23.7E-9	58.8E-9	13
Dov13	6.0E-9	3.5E-9	4
FUOV1	59.4E-6	6.9E-6	3
HeyA8	1.5E-6	2.4E-6	6
IGR-OV1	531.2E-9	1.3E-6	14
IMCC3	942.6E-9	1.1E-6	15
IMCC5	105.1E-9	159.6E-9	20
M41	39.5E-9	18.7E-9	5
M41CSR	37.4E-9	34.4E-9	12
MCAS	56.4E-6	99.8E-6	8
OV2008	383.8E-9	1.1E-6	15
OV90	18.9E-9	11.9E-9	9
Ovary1847	864.6E-9	2.7E-6	19
OVCA420	12.7E-6	22.0E-6	5
OVCA429	22.2E-9	24.2E-9	5
OVCA432	14.9E-6	25.7E-6	3
OVCA433	9.9E-9	10.9E-9	5
OVCAR10	671.9E-9	2.5E-6	16
OVCAR2	22.0E-9	30.8E-9	17
OVCAR3	6.2E-6	14.0E-6	14
OVCAR4	655.3E-9	870.8E-9	5
OVCAR5	278.3E-9	721.8E-9	17
OVCAR8	272.6E-9	681.6E-9	12
PEO1	134.7E-9	244.5E-9	9
PEO4	536.2E-9	868.6E-9	10
SK-OV-3	16.1E-6	30.5E-6	11
SK-OV-4	3.3E-9	1.6E-9	12
SK-OV-6	3.5E-6	10.4E-6	11
T8	255.6E-9	456.6E-9	9
TOV-112D	44.5E-6	67.3E-6	9
TOV-21G	764.1E-9	1.5E-6	11
Tyknu	4.6E-9	2.8E-9	4
TyknuCisR	8.5E-9	8.4E-9	8

curves were used to test any association between the pathway scores ('high' versus 'low' based on a median value cut-off) and overall survival for patients with OVCA.

Results

Forty-one OVCA cell lines were treated with increasing concentrations of gemcitabine, and the IC_{50} values were determined (Table I). Pearson's correlation test using gemcitabine IC_{50} and OVCA cell line gene expression data identified 131 unique genes to be associated with gemcitabine sensitivity ($p<0.001$; Table II). GeneGo MetaCore™ analysis identified three biological pathways that were represented within the 131 genes associated with gemcitabine sensitivity ($p<0.02$). These molecular signaling pathways included O-glycan biosynthesis (p=0.001), Role of Nek in cell cycle regulation (p=0.005), and Antiviral actions of Interferons (p=0.01). Statistical significance was derived from the total number of genes input into the pathway analysis software, the number of input genes present in a specific pathway, and the actual number of genes in that pathway. Thus, the p-value represents the probability that mapping a set of genes to a particular pathway occurs by chance. The O-glycan pathway demonstrated the highest level of statistical significance in its association with sensitivity to gemcitabine (p=0.001) (Fig. 1).

Expression of the O-glycan pathway is associated with OVCA clinical outcome. Based on the above findings, we utilized PCA to develop gene expression signature scores for the pathways associated with gemcitabine sensitivity *in vitro* (15). In this way, a 34-gene 'O-glycan biosynthesis pathway signature' (OGBPS) (Table III) was generated and evaluated in an independent OVCA genomic dataset (16). Using the median value as a threshold to define high versus low OGBPS score, we identified an association between high OGBPS score and favorable survival (p=0.003; Fig. 2A). A similar association between high OGBPS score and favorable survival was observed in patients who underwent optimal (p=0.002) and suboptimal (approaching significance, p=0.07) cytoreduction (Fig. 2B). Most importantly, OVCA patients with a high OGBPS score who underwent suboptimal cytoreduction had a survival superior to patients with a low OGBPS score who underwent optimal cytoreduction (p=0.003). Interestingly, patients who demonstrated a CR to primary platinum-based therapy but had a high OGBPS score had superior survival compared with those patients who demonstrated a CR but had a low OGBPS score (p=0.003) (Fig. 2C). Patients who had an IR to primary therapy had no difference in survival associated with tumor OGBPS score (p=0.653) (Fig. 2D). When evaluated with cytoreductive status, grade, and age, the OGBPS score was an independent variable associated with survival ($p<0.001$).

No associations with survival were observed for the first PCA score for the Role of Nek in cell cycle regulation (59 genes, p=0.3107) or the Antiviral actions of Interferons pathway (66 genes, p=0.5411).

Discussion

In this analysis, we applied an *in vitro* and *in vivo* genome-wide approach to define the molecular underpinnings of OVCA gemcitabine sensitivity. We identified genes and molecular signaling pathways associated with OVCA sensitivity to gemcitabine and, in doing so, have identified the OGBPS to be associated with *in vitro* gemcitabine response and also overall survival from OVCA.

Table II. Genes associated with *in vitro* gemcitabine chemoresistance.

Probe set ID	Gene name	Gene description	Score	p-value
ENST00000376242_at	PSORS1C3	PSORS1C3, AB023059.1	0.785	1.22E-09
AK123047_a_at	NR3C2	NR3C2, MGC133092, MLR, MR, MCR	0.749	1.72E-08
ENST00000366558_a_at	KMO	KMO, dJ317G22.1	0.728	6.82E-08
NM_152772_at	TCP11L2	t-complex 11 (mouse) like 2	0.700	3.61E-07
NM_003890_at	FCGBP	Human IgG Fc binding protein	0.688	6.62E-07
NM_021936_at	PAPPA2	Pregnancy-associated plasma preproprotein-A2	0.680	9.89E-07
NM_139173_s_at	NHEDC1	Na^+/H^+ exchanger domain CG10806-like	0.676	1.25E-06
NM_152888_s_at	COL22A1	Collagen, type XXII, alpha 1	0.656	3.29E-06
NM_016242_at	EMCN	Endomucin, endomucin-2	0.654	3.60E-06
AL133118_at	MAPKSP1	MAPKSP1, MAPBP, MP1, MAP2K1IP1	0.638	7.26E-06
NM_030923_s_at	TMEM163	Transmembrane protein 163	0.636	8.00E-06
NM_024013_at	IFNA1	IFNA1, IFL, IFN, IFN-α, IFNA13, IFN α-D, LeIF D	0.631	9.60E-06
NM_199235_at	COLEC11	Collectin sub-family member 11	0.626	1.18E-05
NM_003585_at	DOC2B	Double C2-like domains, β	0.620	1.55E-05
NM_005472_at	KCNE3	Cardiac voltage-gated K channel accessory	0.618	1.65E-05
NM_194309_at	C21orf125	C21orf125, PRED49, FLJ38036	0.618	1.67E-05
ENST00000260323_at	UNC13C	unc-13 homolog C	0.616	1.82E-05
ENST00000234725_at	TMEM48	Transmembrane protein 48	-0.612	2.09E-05
NM_198058_at	ZNF266	Zinc finger protein 266	-0.603	3.06E-05
AW510703_at	SLC15A4	Solute carrier family 15, member 4	0.601	3.20E-05
NM_020119_at	ZC3HAV1	Zinc finger antiviral protein	-0.597	3.76E-05
NM_019104_s_at	LIN37	lin-37 homolog	0.596	3.91E-05
NM_022774_at	DEM1	DEM1, FLJ11445, FLJ13183, FLJ21144, C1orf176	-0.596	3.92E-05
AA723953_at	SGCD	Sarcoglycan, delta (35 kDa dystrophin-associated glycan)	0.591	4.82E-05
NM_012253_s_at	TKTL1	Transketolase-like 1	0.590	4.87E-05
NM_175613_a_at	CNTN4	Axonal cell adhesion molecule contactin 4	0.590	4.97E-05
NM_006198_at	PCP4	Purkinje cell protein 4	0.589	5.01E-05
NM_012391_at	SPDEF	Human prostate specific Ets, PDEF	0.588	5.25E-05
AK124251_at	LHFPL3	LHFP-like protein 3	0.586	5.65E-05
AK024279_a_at	WIPI2	WD repeat domain, phosphoinositide interacting 2	-0.583	6.38E-05
N25888_a_at	GDF15	Growth differentiation factor 15	0.581	6.72E-05
NM_000705_at	ATP4B	ATPase, H^+/K^+ transporting, beta polypeptide	0.578	7.57E-05
AK097996_at	GALNT2	Polypeptide N-acetylgalactosaminyltransferase 2	-0.577	7.71E-05
NM_014848_at	SV2B	Synaptic vesicle protein 2B	0.577	7.96E-05
AL049464_at	THSD4	Thrombospondin, type I, domain containing 4	0.576	8.03E-05
BM668558_at	SART1	Squamous cell carcinoma antigen recognized by T c	-0.576	8.23E-05
CR606639_a_at	ZFP57	Zinc finger protein 57	0.574	8.62E-05
NM_018053_at	XKR8	X Kell blood group precursor-related family	-0.574	8.73E-05
NM_002239_at	KCNJ3	Subfamily, potassium inwardly-rectifying channel J3	0.573	9.09E-05
BC009808_at	NBR1	Neighbor of BRCA1 gene 1 protein	0.573	9.18E-05
ENST00000360944_s_at	RBAK	RB-associated KRAB repressor	-0.572	9.19E-05
AK023318_s_at	CBARA1	Calcium binding atopy-related autoantigen 1	0.570	9.94E-05
BQ574912_s_at	TOMM5	TOMM5, C9orf105, RP11-263I4.1, Tom5, bA613M10.3	-0.565	0.0001177
ENST00000361262_at	SMC5	Structural maintenance of chromosomes 5	-0.563	0.0001256
ENST00000369578_a_at	ZNF292	Zinc-finger domain protein	0.563	0.000126
BC050372_a_at	OLAH	Oleoyl-ACP hydrolase	0.563	0.0001284
NM_172238_at	TFAP2D	Transcription factor AP-2 β	0.563	0.0001288
NM_134266_at	SLC26A7	Solute carrier family 26, member 7	0.562	0.0001305
BC027487_at	C15orf62		0.561	0.0001364

Table II. Continued.

Probe set ID	Gene name	Gene description	Score	p-value
DC311076_a_at	PIP4K2A	Phosphatidylinositol-4-phosphate 5-kinase type-2	0.561	0.0001374
NM_006786_at	UTS2	Human urotensin II	0.559	0.0001448
BC036592_at	GABRB2	Gamma-aminobutyric-acid receptor beta-2 subunit	0.557	0.0001555
NM_018667_at	SMPD3	Sphingomyelin phosphodiesterase 3	0.554	0.0001718
NM_014717_at	ZNF536	Zinc finger protein 536	0.552	0.000184
NM_014629_s_at	ARHGEF10	Rho guanine nucleotide exchange factor 10	-0.552	0.000185
NM_001005212_at	OR9Q1	Olfactory receptor, family 9, subfamily Q	-0.552	0.0001851
CR603904_s_at	EIF2AK2	Protein kinase RNA-regulated (EIF2AK1)	-0.550	0.0001982
BC050525_at	USP1	Ubiquitin-specific processing protease 1	-0.549	0.0002021
AK024011_at	TOE1	Target of EGR1	-0.547	0.0002146
NM_001037165_s_at	FOXK1	Forkhead box K1	-0.547	0.0002163
DW432944_at	C4orf36	C4orf36, hypothetical protein LOC132989, MGC26744, Hs.507712	0.547	0.0002164
NM_001551_at	IGBP1	Immunoglobulin-binding protein 1	0.546	0.0002189
BX091412_at	KLHL34	KLHL34, kelch-like 34, MGC125650, RP11-450P7.3, FLJ34960	-0.546	0.0002246
R37641_at	CA10	Carbonic anhydrase-related protein 10	0.545	0.0002306
NM_000343_at	SLC5A1	Human Na^+/glucose cotransporter 1 mRNA	0.545	0.0002323
BG776661_at	C10orf104	C10orf104, FLJ33728	0.543	0.0002473
BC122561_at	LIN7A	Lin-7 homolog A	0.542	0.0002521
NM_016486_at	TMEM69	Transmembrane protein 69	-0.541	0.0002638
M18414_at	TRDV1	TRDV1, hDV101S1	0.541	0.000264
NM_014503_at	UTP20	UTP20, down-regulated in metastasis	-0.539	0.0002797
AY153484_at	PAX2	Paired box gene 2	0.537	0.0002962
BU589560_at	CLDN12	CLDN12, claudin 12	0.536	0.0003033
NM_001422_s_at	ELF5	ELF5, ESE2, ESE-2	0.536	0.0003043
BC038514_a_at	DPP10	Dipeptidyl peptidase 10	0.536	0.0003078
BX649183_at	IVNS1ABP	Influenza virus NS1A binding protein	0.531	0.0003515
NM_032588_at	TRIM63	Muscle specific ring finger protein 1	0.531	0.0003543
NM_153705_at	KDELC2	KDELC2, MGC33424, KDEL (Lys-Asp-Glu-Leu) containing 2	-0.531	0.0003585
BX647977_a_at	RNMT	Human RNA (guanine-7-)methyltransferase	0.530	0.0003622
NM_032525_at	TUBB6	Tubulin beta-6 chain	-0.530	0.0003656
NM_017983_at	WIPI1	Human WD-repeat protein interacting with phosphol	0.530	0.0003692
NM_003101_at	SOAT1	Sterol O-acyltransferase 1	-0.530	0.0003695
NM_182538_at	SPNS3	SPNS3, spinster homolog 3, MGC29671	0.529	0.0003766
BU730580_at	RHO	Rhodopsin	0.528	0.0003879
AL713688_s_at	hCG_2009921	hCG_2009921, LOC441204	0.527	0.0003942
NM_016426_at	GTSE1	GTSE1, G-2 and S-phase expressed 1	-0.526	0.000407
DB377031_x_at	PSG4	Pregnancy specific β-1-glycoprotein 4	0.526	0.0004144
BC101614_a_at	WDR72	WD repeat domain 72	0.523	0.0004451
BI761936_a_at	C12orf69		0.522	0.0004594
NM_021808_at	GALNT9	Polypeptide N-acetylgalactosaminyltransferase 9	0.521	0.0004817
NM_022127_at	SLC28A3	Concentrative Na^+-nucleoside cotransporter	0.520	0.00049
AK098151_at	PDK4	Pyruvate dehydrogenase kinase 4	0.519	0.0005028
NM_174900_at	ZFP42	Zinc finger protein 42	0.519	0.0005127
BC035128_a_at	MXI1	MAX interacting protein 1	0.519	0.0005142
NM_001085_at	SERPINA3	Serine proteinase inhibitor, clade A, member 3	0.516	0.0005467
AL564246_at	ZNF277	Zinc finger protein 277	0.516	0.0005478
NM_002813_at	PSMD9	Proteasome 26S non-ATPase subunit 9	-0.515	0.0005733
NM_005318_at	H1F0	H1 histone family, member 0	-0.515	0.0005758
AL136587_at	AGPAT5	1-acylglycerol-3-phosphate O-acyltransferase 5	-0.514	0.0005852

Table II. Continued.

Probe set ID	Gene name	Gene description	Score	p-value
NM_015474_at	SAMHD1	SAM domain- and HD domain-containing protein 1	-0.514	0.0005942
AV708719_at	FAM65C	FAM65C, dJ530I15.2, FLJ00360, FLJ32230, C20orf175	0.513	0.0006068
AF313619_at	PAQR8	Lysosomal membrane protein in brain 1	0.513	0.0006086
NM_005656_at	TMPRSS2	Transmembrane protease, serine 2 catalytic chain	0.513	0.0006113
CN310658_s_at	FXYD6	FXYD domain-containing ion transport regulator 6	0.512	0.000615
NM_032609_s_at	COX4I2	Cytochrome c oxidase subunit 4 isoform 2	0.509	0.0006842
NM_007168_at	ABCA8	ATP-binding cassette, sub-family A member 8	0.507	0.00071
NM_012478_at	WBP2	WW domain binding protein 2	0.507	0.0007162
AK125857_at	NUP62	Nuclear pore glycoprotein p62	-0.507	0.0007163
NM_000078_at	CETP	Cholesteryl ester transfer protein	0.507	0.0007259
NM_001102610_a_at	TUBGCP5	Tubulin, gamma complex associated protein 5	-0.505	0.0007604
NM_005773_at	ZNF256	Zinc finger protein 256	-0.505	0.0007613
CB852298_at	CHORDC1	Chord domain-containing protein 1	-0.505	0.0007663
NM_024306_at	FA2H	Fatty acid hydroxylase domain containing 1	0.504	0.0007716
NM_031891_a_at	CDH20	Cadherin 20	0.503	0.000811
NM_020380_at	CASC5	Cancer susceptibility candidate 5	-0.502	0.0008354
NM_003417_at	ZNF264	Zinc finger protein 264	-0.501	0.000841
NM_018840_at	C20orf24	C20orf24, PNAS-11, RAB5-interacting protein, RIP5	-0.501	0.0008587
NM_021269_s_at	ZNF708	Zinc finger protein 15-like 1 (KOX 8)	-0.500	0.0008837
NM_020167_at	NMUR2	Neuromedin U receptor 2	0.499	0.0008887
NM_001112724_at	STK32A	Serine/threonine kinase 32A	0.499	0.0008995
AK075129_s_at	RHOBTB1	Rho-related BTB domain containing 1	0.498	0.0009097
ENST00000357899_a_at	ZBTB44	Zinc finger and BTB domain containing 44	0.498	0.0009199
CR456455_s_at	SERHL	Serine hydrolase-like	-0.498	0.0009238
NM_080717_at	TBX5	T-box transcription factor TBX5	0.498	0.0009268
BC098116_at	ABCA11P	FLJ14297, MGC120309, MGC120310, MGC120312, MGC132744, MGC138274	-0.498	0.0009313
AK026107_a_at	RBM25	RNA binding motif protein 25, RNA-binding motif protein 25	-0.497	0.0009449
LIT1500_s_at	NOL5A	Nucleolar protein 5A	-0.497	0.0009486
AF233261_a_at	OTOR	OTOR, fibrocyte-derived protein, melanoma inhibitory activity-like B protein	0.497	0.0009601
CR610033_a_at	TOM1L1	Target of Myb-like protein 1	0.496	0.0009693
AI144436_at	SF3A3	Spliceosome-associated protein 61, Splicing factor 3A subunit 3	-0.495	0.0009879
AB053232_at	GAL3ST3	Galactose 3'-sulfotransferase, galactose-3-O-sulfotransferase 3	0.495	0.0009897
NM_206915_s_at	NGFRAP1	NGFRAP1, BEX3, DXS6984E, HGR74, NADE, Bex	-0.495	0.0009941

Previous efforts to define the molecular basis of gemcitabine resistance have identified molecules such as deoxycytidine kinase (dCK) (8,17-19), ribonucleotide reductase (20-22), and human equilibrative nucleoside transporter-1 (hENT1) (4,23-26). Decreased activity of dCK, which phosphorylates gemcitabine to its monophosphate form, has previously been reported to be associated with resistance to gemcitabine (8,17-19). Consistent with these data, in our analysis, we demonstrated a negative correlation between OVCA cell line mRNA expression of the dCK gene and increasing gemcitabine resistance (Pearson's correlation: -0.33, p=0.05). Previously, overexpression of the M1 and M2 subunits of ribonucleotide reductase (RRM1 and RRM2) has been demonstrated to be associated with gemcitabine resistance in gastrointestinal cancer cells (27,28). In our analysis, we observed no association between gemcitabine resistance and expression of RRM1, although we observed an association between low levels of RRM2 expression (using median expression as a threshold) and high gemcitabine IC_{50} ($p<0.02$). It is unclear why our findings are contradictory to those of Davidson *et al* (27); however, they may be due to differences in cancer types studied. Inhibition of hENT1 was previously reported to be associated with gemcitabine chemoresistance (4,25). This correlates with our findings in which we demonstrated a negative correlation between OVCA cell line mRNA expression of the

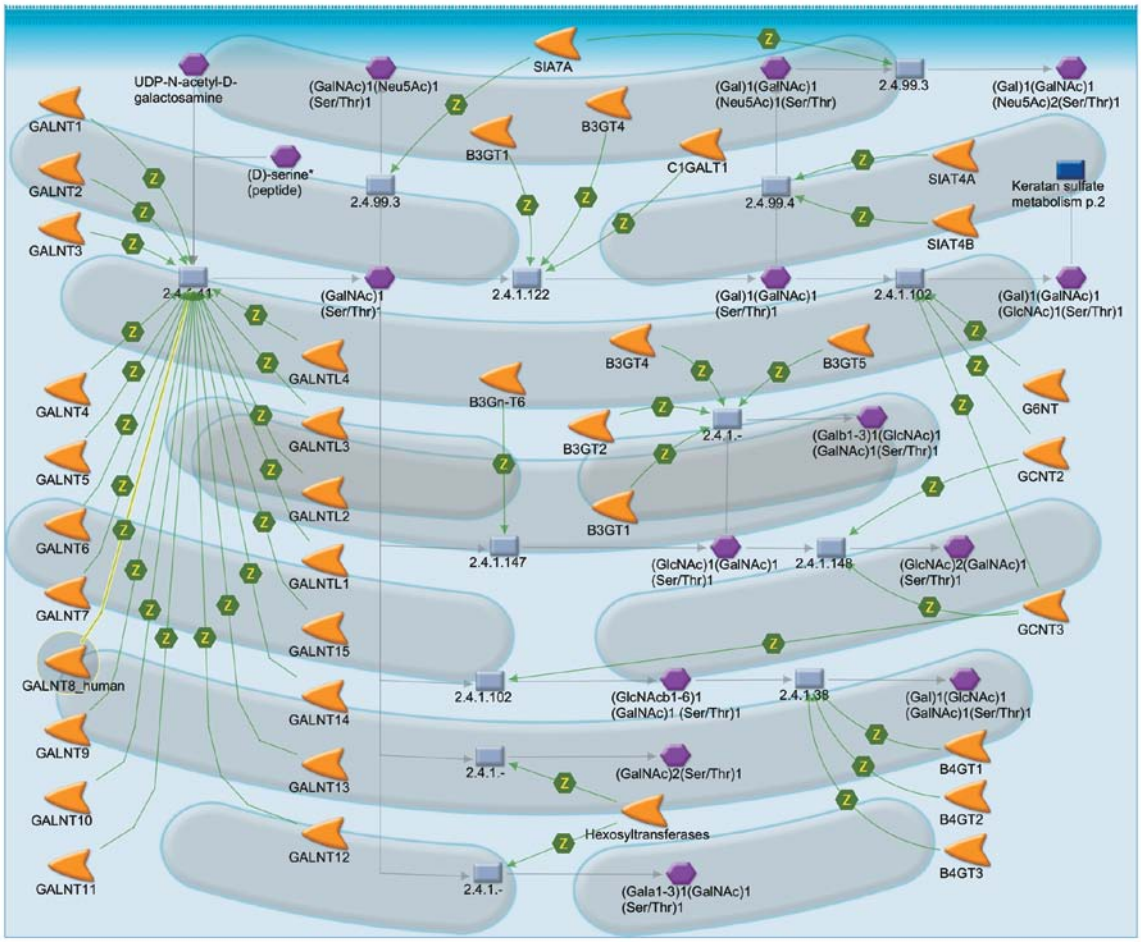

Figure 1. O-glycan biosynthesis/human version pathway.

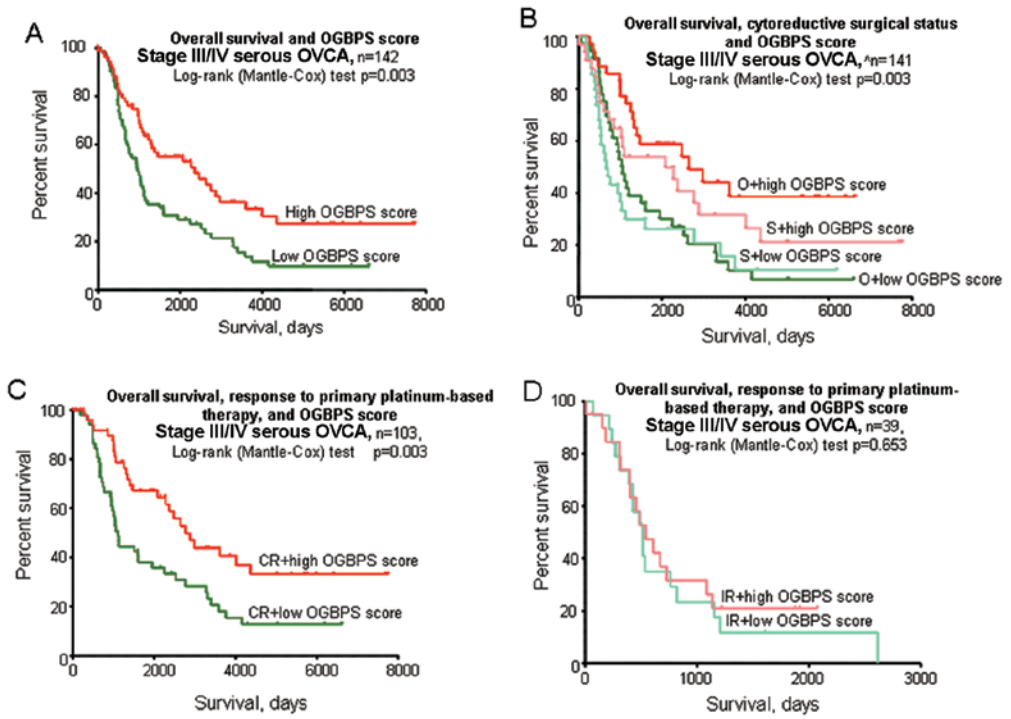

Figure 2. High OGBPS PCA score is associated with favorable clinical outcome. Kaplan-Meier curves depicting the association between OGBPS PCA score and (A) overall survival from OVCA; (B) overall survival and cytoreductive status, (C) overall survival and complete response to platinum therapy median cutoff, and (D) overall survival and incomplete response to platinum therapy. ^Information available for 141 of 142 samples from advanced Stage II/IV serous OVCA datasets. The numbers at risk are shown at the top of graphs. Log-rank test p-values indicate significance. CR, complete response; IR, incomplete response, O, optimal; S, suboptimal.

Table III. OGBPS 34 genes.

NM_020981_at	B3GALT1	Beta-1,3-galactosyltransferase
NM_003783_at	B3GALT2	Beta-1,3-galactosyltransferase, beta-3-galt2
NM_003782_a_at	B3GALT4	Beta-1,3-galactosyltransferase 4
NM_033171_at	B3GALT5	GlcNAc-beta-1,3-galactosyltransferase 5, GLCT5, homolog of C
NM_138706_at	B3GNT6	Beta-1,3-N-acetylglucosaminyltransferase protein
U10474_at	B4GALT1	B4GALT1
NM_003780_at	B4GALT2	B4GALT2
NM_003779_at	B4GALT3	Beta4Gal-T3
NM_020156_at	C1GALT1	Core 1 synthase, glycoprotein-N-acetylgalactosamine
AW798875_at	GALNT1	Polypeptide N-acetylgalactosaminyltransferase 1
NM_024564_at	GALNT10	Polypeptide N-acetylgalactosaminyltransferase 10
NM_022087_at	GALNT11	Polypeptide N-acetylgalactosaminyltransferase 11
AI638649_at	GALNT12	Polypeptide N-acetylgalactosaminyltransferase 12
AK131195_a_at	GALNT13	UDP-N-acetyl-alpha-D-galactosamine:polypeptide
NM_024572_s_at	GALNT14	Polypeptide N-acetylgalactosaminyltransferase 14
AK097996_at	GALNT2	Polypeptide N-acetylgalactosaminyltransferase 2
BX647473_a_at	GALNT3	Polypeptide N-acetylgalactosaminyltransferase 3
NM_003774_at	GALNT4	Polypeptide N-acetylgalactosaminyltransferase 4
BX097451_s_at	GALNT5	Polypeptide N-acetylgalactosaminyltransferase 5
BU542820_at	GALNT6	Polypeptide N-acetylgalactosaminyltransferase 6
NM_017423_at	GALNT7	Polypeptide N-acetylgalactosaminyltransferase 7
BM719843_a_at	GALNT8	N-acetylgalactosaminyltransferase 8
NM_021808_at	GALNT9	Polypeptide N-acetylgalactosaminyltransferase 9
NM_020692_at	GALNTL1	Polypeptide N-acetylgalactosaminyltransferase 16
BC030625_at	GALNTL2	Polypeptide N-acetylgalactosaminyltransferase 13
NM_198516_at	GALNTL4	UDP-N-acetyl-alpha-D-galactosamine
NM_145292_at	GALNTL5	UDP-N-acetyl-alpha-D-galactosamine
NM_001490_at	GCNT1	Beta-1,6-N-acetylglucosaminyltransferase 1
NM_145649_s_at	GCNT2	Beta-1,6-N-acetylglucosaminyltransferase 2
NM_004751_at	GCNT3	Beta1,6-N-acetylglucosaminyltransferase 3
CR619813_at	ST3GAL1	3-Sialyltransferase,Gal-NAc6S
AK127322_at	ST3GAL2	Beta-galactoside alpha-2,3-sialytransferase
NM_018414_at	ST6GALN	6-Sialyltransferase I alpha-N-acetylgalactosaminide alpha-2
BC067524_a_at	WBSCR17	Polypeptide N-acetylgalactosaminyltransferase, Williams-Beuren syndrome chromosome region 17

hENT1 gene and increasing gemcitabine resistance (Pearson's correlation: -0.3, p=0.06).

The process of glycosylation involves the enzymatic addition of carbohydrates to proteins or lipids and is the most common form of post-translational modification. Three categories of protein-linked glycans exist, including those linked to the amide group of asparagine (N-linked), those linked to the hydroxyl group of serine, threonine, or hydroxylysine 3 (O-linked), and those linked to a carboxyl group of tryptophan (C-linked) (29). The main pathway for complex O-glycan biosynthesis is located in the endoplasmic reticulum and Golgi compartments, restricting glycosylation largely to the endoplasmic reticulum, Golgi, lysosomal, plasma membrane, and secretory proteins, with the exception of nuclear and cytosolic proteins, which can be modified with a single O-linked GlcNAc (30). O-glycans have been reported to have a broad range of functions in protein structure and stability, immunity, receptor-mediated signaling, non-specific protein interactions, modulation of the activity of enzymes and signaling molecules, and protein expression and processing (30,31). Although these biological roles range in importance, they can be critical for development, growth, function, and survival. Moreover, a specific O-glycan may influence a range of functions at different locations and times within an organism (31). Previously, limited access to endoglycosidases to cleave intact O-glycans from their protein backbone, as well as the extreme diversity of their structures, has limited research relative to study of N-linked glycan pathway-linked diseases (historically considered the congenital disorders of

glycosylation). More recently, in human cancers, O-glycans have been shown to play important roles in cancer cell attachment, signaling, invasion (32-35), and survival in the bloodstream. Inhibition of the O-glycan pathway in colorectal cancer cell lines has been shown to inhibit cell growth and induce apoptosis (36). Down-regulation of the N-glycan biosynthesis pathway was also reported to be associated with chemoresistance in cholangiocarcinoma cell lines (37).

To date, we are unaware of any reports suggesting that the O-glycan pathway influences OVCA cell response to therapeutic interventions or overall survival. In this study, expression of the O-glycan pathway (quantified by a OGBPS score) was associated with OVCA overall survival when we analyzed: a) all patients with OVCA, b) patients who underwent optimal OVCA surgical cytoreduction, and c) patients who experienced a CR to primary surgery plus platinum-based therapy. The association between OGBPS score and overall survival for patients who underwent suboptimal surgical cytoreduction did not reach statistical significance ($p=0.07$), and no association was identified in patients who experienced an IR to primary surgery plus platinum-based therapy. When evaluated with cytoreductive status, grade, and age, the OGBPS score was an independent variable associated with survival ($p<0.001$). The explanation for the associations between OGBPS and OVCA survival is likely complex. Although in this study we identified the O-glycan pathway by its association with *in vitro* gemcitabine sensitivity, we do not believe that the impact of the pathway on overall survival is driven by its effect of gemcitabine sensitivity. In fact, high OGBPS score was associated with resistance to gemcitabine, yet showed a more favorable outcome for patients with OVCA. As noted above, O-glycans are known to influence cancer cell attachment, signaling, invasion, and survival in the bloodstream (32-35). It is likely that the effect on OVCA clinical outcome is associated with one or more of these important oncologic processes. It will therefore be essential in future studies to investigate associations between OGBPS score, activity of individual members of the O-glycan pathway, and OVCA cell phenotypic behavior.

Our discovery of associations between O-glycan pathway expression and gemcitabine sensitivity and patient survival is novel. These findings potentially have substantial implications for future clinical management of patients with OVCA. In the future, empiric-based treatment decision-making must be replaced with a more tailored strategy that stratifies patients based on their molecular fingerprints. Such an approach will identify those patients with the 'highest risk' disease, those who may benefit from additional pathway-targeted therapy added to standard of care cytotoxic regimens, and potentially those who may (or may not) benefit from aggressive surgical interventions.

Acknowledgements

Opinions, interpretations, conclusions, and recommendations are those of the authors and are not necessarily endorsed by the funding agencies. We thank Rasa Hamilton (Moffitt Cancer Center) for editorial assistance. We also like to thank Merck pharmaceuticals for their contributions. This study was supported in part by the Hearing the Ovarian Cancer Whisper, Jacquie Liggett Foundation, the National Cancer Institute Grant R21 CA-110499-01A2, the Ocala Royal Dames for Cancer Research Inc., the Phi Beta Psi Sorority, the Ovarian Cancer Research Fund, and the US Army Medical Research and Materiel Command under award no. DAMD17-02-2-0051.

References

1. Gadducci A, Sartori E, Maggino T, *et al*: Analysis of failures after negative second-look in patients with advanced ovarian cancer: an Italian multicenter study. Gynecol Oncol 68: 150-155, 1998.
2. McGuire WP, Hoskins WJ, Brady MF, *et al*: Cyclophosphamide and cisplatin compared with paclitaxel and cisplatin in patients with stage III and stage IV ovarian cancer. N Engl J Med 334: 1-6, 1996.
3. Ozols RF: The current role of gemcitabine in ovarian cancer. Semin Oncol 28: 18-24, 2001.
4. Mackey JR, Mani RS, Selner M, *et al*: Functional nucleoside transporters are required for gemcitabine influx and manifestation of toxicity in cancer cell lines. Cancer Res 58: 4349-4357, 1998.
5. Distefano M, Ferlini C, De Vincenzo R, Gaggini C, Mancuso S and Scambia G: Antagonistic effect of the combination gemcitabine/topotecan in ovarian cancer cells. Oncol Res 12: 355-359, 2000.
6. Peters GJ, Bergman AM, Ruiz van Haperen VW, Veerman G, Kuiper CM and Braakhuis BJ: Interaction between cisplatin and gemcitabine in vitro and in vivo. Semin Oncol 22: 72-79, 1995.
7. Ruiz van Haperen VW, Veerman G, Boven E, Noordhuis P, Vermorken JB and Peters GJ: Schedule dependence of sensitivity to 2',2'-difluorodeoxycytidine (Gemcitabine) in relation to accumulation and retention of its triphosphate in solid tumour cell lines and solid tumours. Biochem Pharmacol 48: 1327-1339, 1994.
8. Ruiz van Haperen VW, Veerman G, Eriksson S, *et al*: Development and molecular characterization of a 2',2'-difluorodeoxycytidine-resistant variant of the human ovarian carcinoma cell line A2780. Cancer Res 54: 4138-4143, 1994.
9. Ruiz van Haperen VW, Veerman G, Eriksson S, Stegmann AP and Peters GJ: Induction of resistance to 2',2'-difluorodeoxycytidine in the human ovarian cancer cell line A2780. Semin Oncol 22: 35-41, 1995.
10. Van Moorsel CJ, Veerman G, Bergman AM, *et al*: Combination chemotherapy studies with gemcitabine. Semin Oncol 24 (Suppl 7): 17-23, 1997.
11. Braakhuis BJ, Ruiz van Haperen VW, Boven E, Veerman G and Peters GJ: Schedule-dependent antitumor effect of gemcitabine in in vivo model system. Semin Oncol 22: 42-46, 1995.
12. Friedlander M, Millward MJ, Bell D, *et al*: A phase II study of gemcitabine in platinum pre-treated patients with advanced epithelial ovarian cancer. Ann Oncol 9: 1343-1345, 1998.
13. Lund B, Hansen OP, Theilade K, Hansen M and Neijt JP: Phase II study of gemcitabine (2',2'-difluorodeoxycytidine) in previously treated ovarian cancer patients. J Natl Cancer Inst 86: 1530-1533, 1994.
14. Markman M, Webster K, Zanotti K, Kulp B, Peterson G and Belinson J: Phase 2 trial of single-agent gemcitabine in platinum-paclitaxel refractory ovarian cancer. Gynecol Oncol 90: 593-596, 2003.
15. Chen DT, Nasir A, Culhane A, *et al*: Proliferative genes dominate malignancy-risk gene signature in histologically-normal breast tissue. Breast Cancer Res Treat 119: 335-346, 2010.
16. Marchion DC, Cottrill HM, Xiong Y, *et al*: BAD phosphorylation determines ovarian cancer chemo-sensitivity and patient survival. Clin Cancer Res 17: 6356-6366, 2011.
17. Galmarini CM, Mackey JR and Dumontet C: Nucleoside analogues: mechanisms of drug resistance and reversal strategies. Leukemia 15: 875-890, 2001.
18. Jordheim L, Galmarini CM and Dumontet C: Drug resistance to cytotoxic nucleoside analogues. Curr Drug Targets 4: 443-460, 2003.
19. Van der Wilt CL, Kroep JR, Bergman AM, *et al*: The role of deoxycytidine kinase in gemcitabine cytotoxicity. Adv Exp Med Biol 486: 287-290, 2000.
20. Cory JG and Sato A: Regulation of ribonucleotide reductase activity in mammalian cells. Mol Cell Biochem 53-54: 257-266, 1983.
21. Thelander L and Berg P: Isolation and characterization of expressible cDNA clones encoding the M1 and M2 subunits of mouse ribonucleotide reductase. Mol Cell Biol 6: 3433-3442, 1986.

22. Zhou BS, Tsai P, Ker R, *et al*: Overexpression of transfected human ribonucleotide reductase M2 subunit in human cancer cells enhances their invasive potential. Clin Exp Metastasis 16: 43-49, 1998.
23. Garcia-Manteiga J, Molina-Arcas M, Casado FJ, Mazo A and Pastor-Anglada M: Nucleoside transporter profiles in human pancreatic cancer cells: role of hCNT1 in 2',2'-difluorodeoxycytidine-induced cytotoxicity. Clin Cancer Res 9: 5000-5008, 2003.
24. Mackey JR, Yao SY, Smith KM, *et al*: Gemcitabine transport in xenopus oocytes expressing recombinant plasma membrane mammalian nucleoside transporters. J Natl Cancer Inst 91: 1876-1881, 1999.
25. Rauchwerger DR, Firby PS, Hedley DW and Moore MJ: Equilibrative-sensitive nucleoside transporter and its role in gemcitabine sensitivity. Cancer Res 60: 6075-6079, 2000.
26. Ritzel MW, Ng AM, Yao SY, *et al*: Recent molecular advances in studies of the concentrative Na^+-dependent nucleoside transporter (CNT) family: identification and characterization of novel human and mouse proteins (hCNT3 and mCNT3) broadly selective for purine and pyrimidine nucleosides (system cib). Mol Membr Biol 18: 65-72, 2001.
27. Davidson JD, Ma L, Flagella M, Geeganage S, Gelbert LM and Slapak CA: An increase in the expression of ribonucleotide reductase large subunit 1 is associated with gemcitabine resistance in non-small cell lung cancer cell lines. Cancer Res 64: 3761-3766, 2004.
28. Jung CP, Motwani MV and Schwartz GK: Flavopiridol increases sensitization to gemcitabine in human gastrointestinal cancer cell lines and correlates with down-regulation of ribonucleotide reductase M2 subunit. Clin Cancer Res 7: 2527-2536, 2001.
29. Hofsteenge J, Muller DR, De Beer T, Loffler A, Richter WJ and Vliegenthart JF: New type of linkage between a carbohydrate and a protein: C-glycosylation of a specific tryptophan residue in human RNase Us. Biochemistry 33: 13524-13530, 1994.
30. Wells L and Hart GW: O-GlcNAc turns twenty: functional implications for post-translational modification of nuclear and cytosolic proteins with a sugar. FEBS Lett 546: 154-158, 2003.
31. Varki A: Biological roles of oligosaccharides: all of the theories are correct. Glycobiology 3: 97-130, 1993.
32. Fuster MM, Brown JR, Wang L and Esko JD: A disaccharide precursor of sialyl Lewis X inhibits metastatic potential of tumor cells. Cancer Res 63: 2775-2781, 2003.
33. Gabius HJ: Cell surface glycans: the why and how of their functionality as biochemical signals in lectin-mediated information transfer. Crit Rev Immunol 26: 43-79, 2006.
34. Huet G, Gouyer V, Delacour D, *et al*: Involvement of glycosylation in the intracellular trafficking of glycoproteins in polarized epithelial cells. Biochimie 85: 323-330, 2003.
35. Ulloa F and Real FX: Benzyl-N-acetyl-alpha-D-galactosaminide induces a storage disease-like phenotype by perturbing the endocytic pathway. J Biol Chem 278: 12374-12383, 2003.
36. Patsos G, Hebbe-Viton V, Robbe-Masselot C, *et al*: O-glycan inhibitors generate aryl-glycans, induce apoptosis and lead to growth inhibition in colorectal cancer cell lines. Glycobiology 19: 382-398, 2009.
37. Sato J, Kimura T, Saito T, *et al*: Gene expression analysis for predicting gemcitabine resistance in human cholangiocarcinoma. J Hepatobiliary Pancreat Sci 18: 700-711, 2011.